The holographic glass bead game : from superconductivity to time machines

Bagrov, A.

Chapter 3

Holographic phase diagram of quark-gluon plasma formed in heavy-ions collisions

3.1 Introduction

For the last decade, since the publication of fascinating papers [1–3], it was realized that supersymmetric and non-supersymmetric theories in the strong coupling limit in principle could be pretty close in their properties [4]. The AdS/CFT correspondence, which appeared as a formal duality between the $\mathcal{N} = 4$ super Yang-Mills theory and a quantum gravity in AdS background, has become powerful tool for studying various properties of real physical systems in the strong coupling [5].

Important branch of these investigations is the analysis of the Quark Gluon Plasma (QGP) from the point of view of AdS-holography, see for example, review [6]. These applications of the AdS/CFT correspondence to strongly coupled QGP have been mostly related to equilibrium properties of the plasma, or to its' kinetics/hydrodynamics near the equilibrium.

A particular application of AdS/CFT to the strongly coupled QGP, is the analysis of thermalization of matter and early entropy production instantly after the collision of relativistic heavy ions. RHIC experiments have shown that a QGP forms at a very early stage just after the heavy ion collision, i.e. a rapid thermalization occurs, and QGP produced in RHIC is believed to be strongly coupled as evidenced by its rapid equilibration. Strong collective flows well reproduced by hydrodynamics, and strong jet quenching [7–9]. This obviously requires a calculation of the strongly coupled field theory in non-equilibrium process.

Not long ago Gubser, Yarom and Pufu [11] have proposed the gravi-

tational shock wave in AdS_5 as a possible holographic dual for the heavy ion and have related the area of the trapped surface formed in a collision of such waves to the entropy of matter formed after collision of heavy ions. Early papers where has been mentioned an analogy between colliding heavy ions and colliding gravitational shock waves in anti-de Sitter space include [12]-[16]. This AdS-holographic model has been also used to find the stress-energy tensor of the QGP formed by ion collision. In accordance with AdS/CFT dictonary this stress-energy tensor is dual to the metric of spacetime after collision of shock waves [16].

The main result of [11, 17], confirmed by numerical calculations performed in [18, 19], is that in the limit of a very large collision energy E the multiplicity (the entropy S) grows as

$$S > \mathcal{C}E^{2/3}, \tag{3.1}$$

$\mathcal{C}$ is a numerical factor (see Sect.3.2.1).

Alvarez-Gaume, Gomez, Sabeo Vera, Tavanfar, and Vazquez-Mozoand [20] have considered central collision of shock waves sourced by a nontrivial matter distribution in the transverse space and they have found critical phenomenon occurring as the shock wave reaches some diluteness limit. This criticality may be related to criticality found in [18]. The numerical results of [18] show the existence of a simple scaling relation between the critical impact parameter and the energy of colliding waves.

The size of colliding nuclei is introduced via the distance of those objects from the boundary along the holographic coordinate z.

The model of infinite homogenous wall has been proposed and analyzed by Shuryak and Lin [18]. The advantage of this model is the essential simplicity of calculations. However, the legitimacy of these calculations requires some additional examinations (see our discussion in Sect. 3.2.2).

In heavy ion collisions not only the energy per nucleus is important variable. One can try to associate different nuclei with different kinds of shock waves. There are several proposal in literature on this subject. For example, in [21] the holographic model with cutting off the UV part of the bulk geometry, has been proposed. Formation of trapped surfaces (TS) in head-on collisions of charged shock waves in the (A)dS background has been considered in [22] and it has been shown that the formation of trapped surfaces on the past light cone is only possible when charge is below certain critical value - situation similar to the collision of two ultrarelativistic charges in Minkowski space-time [23]. This critical value

depends on the energy of colliding particles and the value of a cosmological constant. The formation of trapped surfaces in head-on collisions of shock waves in gravitational theories with more complicated bulk dynamics, in particular with the Einstein-dilaton dynamics, pretended to describe holographic physics that is closer to QCD than the pure AdS theory [24, 21], has been considered recently by Kiritsis and Taliotis [25][1] and they have found that the multiplicity grows as

$$S \gtrsim E^{0.24}, \tag{3.2}$$

that is rather close to the experimental data.

In this chapter we propose to incorporate the study of collisions of charged shock gravitational waves [22] into the description of colliding nuclei with non-zero baryon chemical potential. In the holographic context, the chemical potential of strongly coupled QGP on the gravity side is related to temporal component A_t of the $U(1)$ gauge field [27]-[34]. The asymptotic value of this gauge field component in the bulk is interpreted as the chemical potential in the gauge theory

$$\mu = A_t|_{\text{boundary}}. \tag{3.3}$$

We use the same identification (3.3) for colliding ions. It would be interesting to perform calculations for the off-center collision of charged gravitational waves or generally smeared charged shock waves. Postponing this problem for further investigations, here we consider the head-on collision of charged point shock waves and charged wall shock waves. This will give us the holographic picture for QPG phase diagram in the first moment after collisions of heavy ions. This phase diagrams, chemical potential (charge) μ versus temperature (energy) T, are displayed in Fig. 5 and Fig. 11. The colored lines separate the TS-phase from the phase free of TS. Let us note that the obtained diagrams differ from the phase diagram for equilibrium QGP (see Fig.3.1 in Sect. 3.2.1).

The chapter is organized as follows. In Sect.2 we present our set up of the problem. In Sect.2.1.1 we describe the role of black holes in AdS/CFT description of strongly coupled QGP. In Sect. 2.1.2. we present the description of the chemical potential of QGP within the AdS/CFT correspondence. In Sect. 2.1.3 we remind the main facts about shock waves in

[1] Collision of dilatonic shock waves in the flat background has been considered in [26].

AdS_5 related to the trapped surface formation. In Sect.2.1.4 we describe in details the dual conjecture proposed in [11]. In Sect.2.2 we pay a special attention to the problem of regularization that appears within the wall shock waves approach. In Sect. 3 we present the phase diagram, temperature vs chemical potential, for QGP formed in the heavy-ions collisions by using the holographic approach with the central collision of charged shock waves. In Sect. 4 we present our calculations of the same problem by using the regularized version of the charged wall shock waves. We summarize our calculations in Sect. 5 and present here also further directions related to holographic description of quark-gluon plasma formed in heavy-ions collisions.

3.2 Set up

3.2.1 Dual conjectures

Black holes and AdS/CFT correspondence for strongly coupled QGP

The idea of AdS/CFT applications to description of the QGP is based on the possibility to make an one to one correspondence between phenomenological/termodynamical parameters of plasma – T, E, P, μ – and parameters that characterize deformations of AdS_5. In the dual gravity setting the source of temperature and entropy are attributed to the gravitational horizons. The relation between energy density and temperature typical for the BH in AdS according [35, 36] is

$$E = \frac{3\pi^3 L^3}{16 G_5} T^4 \tag{3.4}$$

In the phenomenological model of QGP, such as the Landau or Bjorken hydrodynamical models [37, 38], the plasma is characterized by a space-time profile of the energy-momentum tensor $T_{\mu\nu}(x^\rho)$, $\mu, \nu, \rho = 0, ...3$. This state has its counterpart on the gravity side as a modification of the geometry of the original AdS_5 metric. This follows the general AdS/CFT line: operators in the gauge theory correspond to fields in SUGRA. In the case of the energy-momentum tensor, the corresponding field is just the 5D metric. It is convenient to parameterize corresponding 5-dimensional

geometry as

$$ds^2 = L^2 \frac{g_{\mu\nu}(x^\rho, z)dx^\mu dx^\nu + dz^2}{z^2}, \tag{3.5}$$

that is the 5D Fefferman-Graham metric [39]. The flat case $g_{\mu\nu} = \eta_{\mu\nu}$ parametrizes AdS_5 in Poincaré coordinates. The conformal boundary of space-time is at $z=0$ and

$$g_{\mu\nu}(x^\rho, z) = \eta_{\mu\nu} + z^4 g^{(4)}_{\mu\nu}(x^\rho) + \dots \tag{3.6}$$

The AdS/CFT duality leads to the relation

$$g^{(4)}_{\mu\nu}(x^\rho) \sim < T_{\mu\nu}(x^\rho) > \tag{3.7}$$

Applications of AdS/CFT correspondence to hydrodynamical description of the GQP is based on the fact that the energy momentum tensor can be read off from the expansion of the BH in AdS_5 metric (3.6) corresponding to simple hydrodynamical model

$$< T_{\mu\nu} > \propto g^{(4)}_{\mu\nu} = \mathrm{diag}(3/z_0^4, 1/z_0^4, 1/z_0^4, 1/z_0^4) \tag{3.8}$$

The BH in AdS_5 in the Fefferman-Graham coordinates has the form (3.5) with the following nonzero components of $g_{\mu\nu}(x^\rho, z)$ (see [6] and refs therein)

$$g_{00} = -\frac{\left(1-\frac{z^4}{z_0^4}\right)^2}{\left(1+\frac{z^4}{z_0^4}\right)}, \quad g_{ii} = \left(1+\frac{z^4}{z_0^4}\right) \tag{3.9}$$

A change of coordinates $\tilde{z} = z/(1+z^4/z_0^4)^{1/2}$ transforms (3.5) to the standard metric form of the AdS-Schwarzschild static black hole

$$\tilde{z}^2 ds^2 = -\left(1-\frac{\tilde{z}^4}{\tilde{z}_0^4}\right) dt^2 + d\vec{x}^2 + \frac{1}{1-\frac{\tilde{z}^4}{\tilde{z}_0^4}} d\tilde{z}^2, \tag{3.10}$$

with $\tilde{z}_0 = z_0/\sqrt{2}$ being the location of the horizon.

Chemical potential in QGP via AdS/CFT correspondence

The Reissner-Nordström metric in AdS has the following form:

$$ds^2 = -g(R)dT^2 + g(R)^{-1}dR^2 + R^2 d\Omega^2_{D-2}, \tag{3.11}$$

$$g(R) = 1 - \frac{2M}{R^2} + \frac{Q^2}{R^4} + \frac{\Lambda}{3}R^2, \tag{3.12}$$

where Λ is cosmological constant, $\Lambda/3 \equiv 1/a^2$, M and Q are related to the ADM (Arnowitt-Deser-Misner) mass m and the charge σ

$$M = \frac{4\pi G_5 m}{3\pi^2}, \quad Q^2 = \frac{4\pi G_5 \sigma^2}{3}. \tag{3.13}$$

σ is a charge of the electromagnetic field (pure electric) with only one non-zero component

$$A = A_T dT = \Big(- \sqrt{\frac{3}{4}} \frac{Q}{R^2} + \Phi \Big) dT, \tag{3.14}$$

here Φ is a constant $\Phi = \frac{\sqrt{3}}{2}\frac{Q}{R_+^2}$, where R_+ is the largest real root of $g(R)$. Thermodynamics of the charged BH is described by the grand canonical potential (free energy) $W = I/\beta$, the Hawking temperature $T = 1/\beta$, and the chemical potential [40, 41] that are given by

$$I = \frac{\pi\beta}{8G_5 a^2}\left(a^2 R_+^2 + R_+^4 - \frac{Q^2 a^2}{R_+^2}\right), \quad T = \frac{1}{4\pi} g'(R_+), \quad \mu = \frac{\sqrt{3}Q}{2R_+^2}, \tag{3.15}$$

here R_+ is outer horizon, $g(R_+) = 0$, I is given by the value of the action at (3.12) and (3.14). The relation with the first low of thermodynamics, $d\mathcal{E} = Td\mathcal{S} + \mu d\mathcal{Q}$ is achieved under identification

$$W = \mathcal{E} - T\mathcal{S} - \Phi\mathcal{Q}, \quad \mathcal{E} = m, \quad \mathcal{S} = \frac{S_H}{4G_5}, \quad \mathcal{Q} = q, \quad \mu = \Phi \tag{3.16}$$

Note that just the asymptotic value of a single gauge field component gives the chemical potential [27]-[34]

$$\mu = \lim_{r\to\infty} A_t(r) \tag{3.17}$$

The QGP is characterized at least by two parameters: temperature and chemical potential. Generically speaking, quantum field theories may have non zero chemical potentials for any or all of their Noether charges. Within the AdS/CFT context two different types of chemical potential are considered, namely related to the R charge and to baryon number.

Baryon number charge can only occur when we have a theory containing fundamental flavours. Introduction flavours into the gauge theory

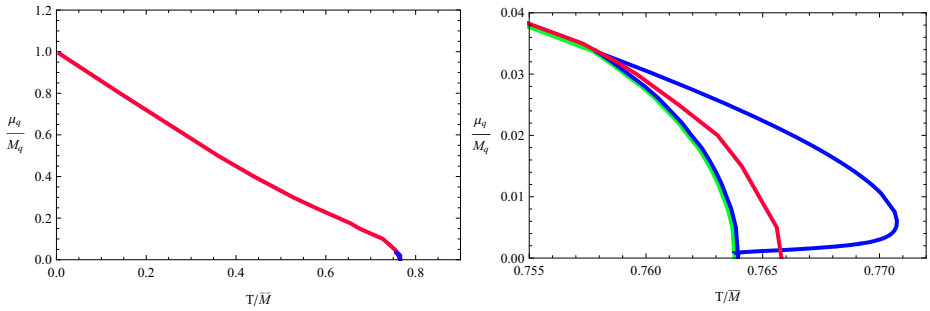

(a) (b)

Figure 3.1. Phase diagram from [27]: Quark chemical potential μ_q/M_q, in versus temperature $T/\bar{M}$. The red line separates the phase of Minkowski embeddings (small temperatures, small μ_q/M_q) from black hole embeddings (see details in [27]). Figure (b) zooms in on the region near the end of this line. Different lines in (b) correspond to different embedding geometries.

by means of a D7 brane leads to appearance of a $U(N_f)$ global flavour symmetry. The flavour group contains a $U(1)_B$, that is a baryon number symmetry, and for this baryon number one adds a chemical potential μ_b [28]. To calculate the free energy one has to calculate the DBI action for a D7 brane. Note that there is a divergence in formal definition, so we must go through the process of renormalization, see for example lectures [42] and for yearly discussion [43].

R charge chemical potential appears for SUSY models [34]. In the N = 1 case there is a U(1) R symmetry group. As to extended SUSY, say N=2, the quark mass term breaks R symmetry.

The typical phase diagram the chemical potential vs the temperature is presented in Fig. 3.1 (the diagram is taken from [27]). In the phase diagram: $\mu_q = \dfrac{\mu_b}{N_c}$, μ_q is the quark chemical potential and $\bar{M} \propto m_q$ is a mass scale defined as $\bar{M} = 2M_q/\sqrt{\lambda}$ and $\lambda = g^2_{YM}N_c$.

Shock waves in AdS$_5$

Shock waves propagating in AdS have the form

$$ds^2 = L^2 \frac{-dudv + dx_\perp^2 + \phi(x_\perp, z)\delta(u)du^2 + dz^2}{z^2}, \qquad (3.18)$$

where u and v are light-cone coordinates, and $x_\perp$ are coordinates transversal to the direction of motion of the shock wave and to z-direction. This metric is sourced by the stress-energy momentum tensor T_{MN} with only one non-zero component T^{SW}_{uu}

$$T^{SW}_{uu} = J_{uu}(z, x_\perp)\delta(u) \tag{3.19}$$

and the Einstein E.O.M. reduces to

$$(\Box_{H_3} - \frac{3}{L^2})\Phi(z, x_\perp) = -16\pi G_5 \frac{z}{L} J_{uu}(z, x_\perp) \tag{3.20}$$

where

$$\Phi(z, x_\perp) \equiv \frac{L}{z}\phi(z, x_\perp) \tag{3.21}$$

and

$$\Box_{H_3} = \frac{z^3}{L^2}\frac{\partial}{\partial z} z^{-1} \frac{\partial}{\partial z} + \frac{z^2}{L^2}(\frac{\partial^2}{\partial x_\perp^2}) \tag{3.22}$$

Different forms of the shock waves correspond to different forms of the source $J_{uu}(z, x_\perp)$. The most general $O(3)$ invariant shock wave in AdS located at $u = 0$ corresponds to

$$\Phi^{O(3)}(z, x_\perp) = F(q). \tag{3.23}$$

where q is the chordal distance

$$q = \frac{(x^1_\perp)^2 + (x^2_\perp)^2 + (z - z_0)^2}{4 z z_0}, \tag{3.24}$$

In this case ρ, related to J_{uu} as

$$\frac{z}{L} J_{uu}(z, x_\perp) \equiv \rho(z, x_\perp), \tag{3.25}$$

has the form

$$\rho^{O(3)}(z, x_\perp) = \rho(q), \tag{3.26}$$

and the Einstein E.O.M takes the form

$$(\Box_{H_3} - \frac{3}{L^2})F = -16\pi G_5\, \rho(q) \tag{3.27}$$

or explicitly

$$q(q+1)F''_{qq} + (3/2)(1+2q)F'_q - 3F = -16\pi G_5 L^2\, \rho(q), \tag{3.28}$$

The shape of point shock wave F^p is given by the solution to (3.20) with

$$J_{uu} = E\delta(u)\delta(z-L)\delta(x^1)\delta(x^2) \tag{3.29}$$

and has the form is given by

$$F^p(z, x_\perp) = \frac{8L^2 G_5 E z^3}{(x_\perp^2 + (z-L)^2)^3} \tag{3.30}$$

This point shock wave shape is in fact equal to $F^p(q)$, $\Phi^{point}(z, x_\perp) = F^p(q)$, that is a solution to (3.28) with

$$\rho^p(q) = \frac{E}{L^3} \frac{\delta(q)}{\sqrt{q(1+q)}}. \tag{3.31}$$

It has the form

$$F^p = \frac{2G_5 E}{L} \left(\frac{(8q^2+8q+1) - 4(2q+1)\sqrt{q(1+q)}}{\sqrt{q(1+q)}} \right) \tag{3.32}$$

The shape of the charged point shock wave is a sum of two components

$$F = F^p + F^Q \tag{3.33}$$

where F^p is given by (3.32) and F^Q is the solution to (3.28) with

$$\rho^{pQ} = \frac{5\bar{Q}^2}{32 \cdot 64\, L^5 G_5} \frac{1}{[q(q+1)]^{5/2}} = \frac{5Q_n^2}{\pi 24 \cdot 64\, L^5} \frac{1}{[q(q+1)]^{5/2}}, \tag{3.34}$$

explicitly

$$F^Q = \frac{5G_5 Q_n^2}{48L^3} \frac{144q^2 + 16q - 1 + 128q^4 + 256q^3 - 64(2q+1)q(q+1)\sqrt{q(1+q)}}{q(1+q)\sqrt{q(1+q)}} \tag{3.35}$$

To establish the connection with [22] let us note the relations of notations

$$\bar{M} = \frac{4G_5 E}{3\pi} \tag{3.36}$$

$$\bar{Q}^2 = \frac{4G_5 Q_n^2}{3\pi} \tag{3.37}$$

and

$$\frac{3\pi\bar{M}}{2a} = \frac{2G_5E}{L} \tag{3.38}$$

$$\frac{5\pi\bar{Q}^2}{64a^3} = \frac{5G_5Q_n^2}{48L^3} \tag{3.39}$$

More complicated shock waves in AdS and dS have been considered in [44–49].

GYP dual conjecture

Gubser, Yarom and Pufu (GYP) [11] have proposed the following dual to QCD holographic picture for colliding nuclei:

- the bulk dual of the boundary nuclei is the shock waves propagating in AdS of the form (3.18);
- the bulk dual of two colliding nuclei in the bulk is the line element for two identical shock waves propagating towards one another in AdS

$$ds^2 = L^2\frac{-dudv + dx_\perp^2 + \phi_1(x_\perp, z)\delta(u)du^2 + +\phi_2(x_\perp, z)\delta(v)dv^2 + dz^2}{z^2}; \tag{3.40}$$

- when the shock waves collide in the bulk, a black hole should form, signifying the formation of a quark-gluon-plasma.

To estimate the BH formation one usually use the TS technic [50, 51].[2] A trapped surface is a surface whose null normals all propagate inward [53]. There is no rigorous proof that the TS formation in asymptotically AdS spacetime provides the BH formation, however there is an common belief that trapped surfaces must lie behind an event horizon and that a lower bound on entropy S_{AdS} of the black hole is given by area of the TS, $A_{trapped}$,

$$S_{AdS} \geq S_{trapped} \equiv \frac{A_{trapped}}{4G_5} \tag{3.41}$$

[2] This estimation can be also performed using so-called capture arguments [52, 26].

To make the proposed duality prescription more precise one has to fix the relations between the bulk parameters, G_5, L, E and the phenomenological parameters of QGP. According to [21], one of these relations is

$$\frac{L^3}{G_5} = \frac{16E \cdot T^4}{3\pi^3} = \frac{11 \cdot 16}{3\pi^3} \approx 1.9 \tag{3.42}$$

The arguments supporting (3.42) are following. Lattice calculations in QGP [57] have shown that ET^4 is a slowly varied quantity and

$$ET^4 \approx 11. \tag{3.43}$$

Just to match the black hole equation of state (3.4) with (3.43), Gubser, Yarom and Pufu [11] have assumed (3.42). It is important to note that here is assumed an identification of the total energy of each nucleus with the energy of the corresponding shock wave. One can modify this identification and assume that only a part of energy of the gravitational shock wave is related to the total energy of nucleus.

To fix the dimensionless parameter EL the AdS/CFT dual relation (3.7) between the expectation value of the gauge theory stress tensor and the AdS_5 metric deformation by the shock wave has been used [11],

$$\langle T_{uu} \rangle = \frac{L^2}{4\pi G_5} \lim_{z \to 0} \frac{1}{z^3} \Phi(z, x_\perp) \delta(u) \tag{3.44}$$

For the point shock wave Φ^{point} given by (3.30), one gets the following stress tensor in the boundary field theory:

$$\langle T_{uu} \rangle = \frac{2L^4 E}{\pi (L^2 + (x^1)^2 + (x^2)^2)^3} \delta(u) \tag{3.45}$$

The r.h.s. of (3.45) depends on the total energy E and L, and L has a meaning of the root-mean-square radius of the transverse energy distribution. It has been assumed [11] that L is equal to the root-mean-square transverse radius of the nucleons, that is in according with a Woods-Saxon profile for the nuclear density [54, 55] is of order of few fm. In particular for Au it is equal to $L \approx 4.3\,\text{fm}$. For Pb it is $L \approx 4.4\,\text{fm}$.

The RHIC collides Au nuclei, (A=197), at $\sqrt{s_{NN}} = 200\,\text{GeV}$. This means that each nucleus has energy $E = 100\,\text{GeV}$ per nucleon, for a total of about $E = E_{\text{beam}} = 19.7\,\text{TeV}$ for each nucleus.

LHC will collide Pb nuclei, (A=208) at $\sqrt{s_{NN}} = 5.5\,\text{TeV}$, that means $E = E_{\text{beam}} = 570\,\text{TeV}$.

Estimations of [11] for dimensionless values EL for Au-Au and Pb-Pb collisions are

$$EL|_{Au-Au,\sqrt{s_{NN}}=200\,\mathrm{GeV}} \approx 4.3\times 10^5\,, \tag{3.46}$$

$$EL|_{Au-Au,\sqrt{s_{NN}}=5.5\,\mathrm{TeV}} \approx 1.27\times 10^7\,, \tag{3.47}$$

Note, that in [18] has been proposed to tune the scale L or z_0 of the bulk colliding object to the size of the nucleus, or to the "saturation scale" Q_s in the "color glass" models.

Calculations in [11] show that in the limit of a very large collision energy E the entropy grows as $E^{2/3}$,

$$S_{\mathrm{trapped}} \approx \pi \left(\frac{L^3}{G_5}\right)^{1/3} (2EL)^{2/3}, \tag{3.48}$$

Considerations of off-center collisions of gravitational shock waves in AdS do not change the scaling $E^{2/3}$. However, a critical impact parameter, beyond which the trapped surface does not exist has been observed [18] (compare with result of [20]). Experimental indications for similar critical impact parameter in real collisions have been noted [18].

The relation of the total multiplicity, S_{QGP}, given by experimental data, and the entropy produced in the gravitational waves collision in AdS_5, S_{AdS} has some subtleties [21]. Phenomenological considerations [56, 58, 11], estimate the total multiplicity S_{QGP} by the the number of charged particles N_{ch} times the factor ~ 7.5.

$$S_{QGP} \approx 7.5 N_{\mathrm{charged}}. \tag{3.49}$$

The trapped surface analysis does not give the produced entropy but it provides a lower bound

$$S_{trapped} \leq S_{AdS}. \tag{3.50}$$

Taking into account that in calculations [11] the energy of the gravitational shock wave is identified with the energy of colliding ions and L with the nucleus size, one can introduce proportionality constants between these quantities to get

$$\mathcal{M} \cdot S_{trapped} < N_{\mathrm{charged}} \tag{3.51}$$

where all proportionality factors are included into the overall factor $\mathcal{M}$. One can take $\mathcal{M}$ to fit the experimental data at some point. But the

scaling $S_{\text{trapped}} \propto s_{NN}^{1/3}$ implied by (3.48) differs from the observed scaling, which is closer to the dependence $S \propto s_{NN}^{1/4}$, that predicted by the Landau model [37], see Fig.3.2. It is obvious, that if $E < E_{max}$ one can avoid a conflict between [11] and experiment, but if E can be arbitrary large the conflict takes place.

In figure 3.2 we plot the dependence of the entropy bound (3.48) on the energy, together with the curve that schematically represents the realistic curve that fits experimental data [59]. We can see that by changing the coefficient $\mathcal{M}$ one can avoid the conflict only for energy up to some E_{max}. The overall coefficient of the numerical plot has been chosen in order to

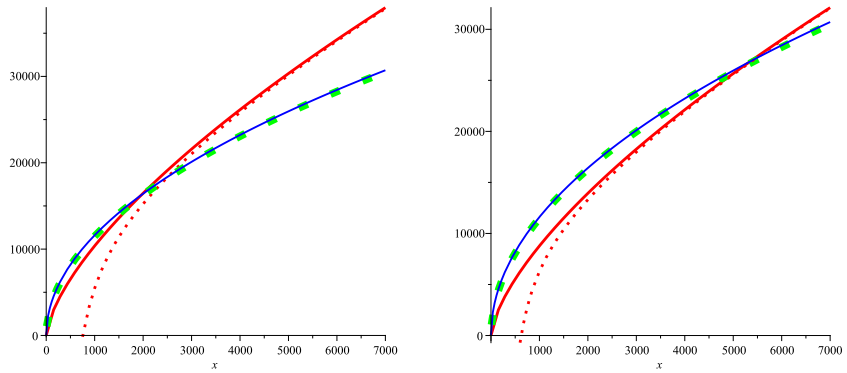

Figure 3.2. (color on-line) Plots of the total number of charged particles vs. energy. The red lines present the estimation (2.45). Plots A and B differ by the overall factor $\mathcal{M}$. The blue lines correspond to the prediction of the Landau model and the dotted green lines schematically present the curves that fit experimental data. The dashed lines correspond to corrections to the GYP multiplicity via non-zero chemical potential, see Sect.3.

fit the RHIC data [59]. Their are indicated by dots in Fig.3.2.

In the above estimation energy of each shock wave is identified with the energy of colliding beams. As has been noted in [17] one can improve fit to the data by identifying the energy of each shock wave with the fraction of the energy of the nucleus carried by nucleus that participate in the collision. This give an extra parameter to fit data. But still a conflict will arise at large energies. In paper [17] it has been proposed to cure the problem by removing a UV part of AdS bulk. In [25] shock waves corresponding to the BH with non-zero dilaton field [24] were considered and it has been shown that lower bound on N_{charged} scales is rather closer

to $s_{NN}^{1/4}$.

3.2.2 Remarks about the regularization of TS calculations in the case of wall-on-wall collisions

In [18] has been proposed a much simpler dual description of the colliding nuclei that uses a wall-on-wall collision in the bulk. The Einstein equation for the profile of the wall shock wave [18] has the form:

$$(\partial_z^2 - \frac{3}{z}\partial_z)\phi(z) = J_{uu}^{WP}, \quad J_{uu}^{WP} = -16\pi G_5 \frac{E}{L^2}\frac{z_0^3}{L^3}\delta(z - z_0) \tag{3.52}$$

To find a trapped surface that can be formed in the collision of two wall shock waves one needs to find a solution to the Einstein eq.(3.52) that satisfies two conditions. It is convenient to write these conditions in terms of function $\psi(z)$ related to ϕ via

$$\phi(z) = \frac{z}{L}\psi. \tag{3.53}$$

They have the form

$$\psi(z_a) = \psi(z_b) = 0, \tag{3.54}$$

$$\psi'(z_a)\frac{z_a}{L} = 2, \qquad \psi'(z_b)\frac{z_b}{L} = -2 \tag{3.55}$$

where z_a, z_b are supposed to be the boundaries of the trapped surface [18]. But as we will see in the moment, strictly speaking, one cannot call the solution to the equation (3.52) with b.c. (3.54) and (3.55) the trapped surface, since by definition this surface supposed to be smooth and compact meanwhile the solution [18] is *non-smooth* and *noncompact*.

By this reason we call the solution found in [18] a quasi-trapped surface. Let us remind the construction presented in [18].

In [60], the solution to the Einstein equation (3.52) is written in such a way that the property (3.54) is satisfied automatically. This solution has the form

$$\psi(z) = \psi_a(z)\Theta(z_0 - z) + \psi_b(z)\Theta(z - z_0) \tag{3.56}$$

$$\psi_a(z) = -\frac{4\,G\pi\,E\left(\frac{z_0^4}{{z_b}^4} - 1\right){z_b}^4{z_a}^3\left(\frac{z^3}{{z_a}^3} - \frac{z_a}{z}\right)}{L^4\left({z_b}^4 - {z_a}^4\right)}$$

$$\psi_b(z) = -\frac{4\,G\pi\,E\left(\frac{{z_0}^4}{{z_a}^4}-1\right){z_a}^4{z_b}^3\left(\frac{z^3}{{z_b}^3}-\frac{z_b}{z}\right)}{L^4\left({z_b}^4-{z_a}^4\right)}$$

Let us first note that solution (3.56) is not smooth. There is a non-smooth part of the solution (3.56)

$$\Xi = \frac{\mathcal{K}}{z}\left(-\frac{z_b}{z_a^3}\left(\Upsilon_1\right)-\frac{z_a}{z_b^3}\left(\Upsilon_2\right)\right), \quad \text{where} \tag{3.57}$$

$$\Upsilon_1 = z^4\Theta(z_0-z)+z_0^4\Theta(z-z_0) \tag{3.58}$$

$$\Upsilon_2 = z_0^4\Theta(z_0-z)+z^4\Theta(z-z_0) \tag{3.59}$$

where

$$\mathcal{K} = \frac{4\,G\pi\,E}{L^4}\frac{z_a^3 z_b^3}{z_b^4-z_a^4} \tag{3.60}$$

Thus, in order to smooth the solution we have to smooth the function Ξ. We can do it by performing the regularization of the Heaviside step function

$$\Theta(z_0-z) \approx \Gamma_1 = \frac{\arctan\left(R\left(z_0-z\right)\right)^3}{\pi}+\frac{1}{2} \tag{3.61}$$

$$\Theta(z-z_0) \approx \Gamma_2 = \frac{\arctan\left(R\left(z-z_0\right)\right)^3}{\pi}+\frac{1}{2}: \tag{3.62}$$

and considering the regularized functions $\tilde{\Upsilon}_1$ and $\tilde{\Upsilon}_2$

$$\tilde{\Upsilon}_1 = z^4\left(\frac{\arctan\left(R\left(z_0-z\right)\right)^3}{\pi}+\frac{1}{2}\right)+z_0^4\left(\frac{\arctan\left(R\left(z-z_0\right)\right)^3}{\pi}+\frac{1}{2}\right)$$

$$\tilde{\Upsilon}_2 = z_0^4\left(\frac{\arctan\left(R\left(z_0-z\right)\right)^3}{\pi}+\frac{1}{2}\right)+z^4\left(\frac{\arctan\left(R\left(z-z_0\right)\right)^3}{\pi}+\frac{1}{2}\right)$$

For derivatives we have

$$\frac{d\Upsilon_1}{dz} \approx 4z^3\Theta(z_0-z), \frac{d\tilde{\Upsilon}_1}{dz} \approx \frac{4z^3\left(\arctan(R(z_0-z)^3+\pi\right)}{\pi} \tag{3.63}$$

$$\frac{d\Upsilon_2}{dz} \approx 4z^3\Theta(z-z_0), \frac{d\tilde{\Upsilon}_2}{dz} \approx \frac{4z^3\left(\arctan(R(z-z_0)^3+\pi\right)}{\pi} \tag{3.64}$$

In Fig.3.3 we present the derivatives of functions Υ_1, Υ_2 as well as derivatives of the smoothed functions $\tilde{\Upsilon}_1$, $\tilde{\Upsilon}_2$.

For $R = 10^4$ (see below) the differences between derivatives $\frac{d\widetilde{Y}_i}{dz}$ and their approximations given by (3.63) and (3.64)

$$\Delta_1(z) = \frac{d\widetilde{Y}_1}{dz} - \left(\frac{d\widetilde{Y}_1}{dz}\right)_{appr}, \quad \Delta_2(z) = \frac{d\widetilde{Y}_2}{dz} - \left(\frac{d\widetilde{Y}_2}{dz}\right)_{appr} \tag{3.65}$$

$$\Delta_1(z) = -\Delta_2(z) = -3\,\frac{z^4 R^3\,(z_0 - z)^2}{\left(1 + R^6\,(z_0 - z)^6\right)\pi} + 3\,\frac{{z_0}^4 R^3\,(z - z_0)^2}{\left(1 + R^6\,(z - z_0)^6\right)\pi}$$

are of order $\gtrsim 10^{-3}$ fm^3 only in the interval $z \in [z_0', z_0'']$, $z_0' = 4.293$ fm, $z_0'' = 4.307$ fm.

Indeed, in our consideration (spread case) the largest value of z_a is 4.260706906 fm and the smallest value of z_b is 4.340400579 fm. At the points $z_0' = 4.260706906$ fm, $z_0'' = 4.340400579$ fm the quantity Δ_1 is less then $\leq 5 \cdot 10^{-6}$ fm^3.

At the points $z_0' = 0.6948439783$ fm, $z_0'' = 1018.393720$ fm the quantity Δ_1 is less then $\leq 2 \cdot 10^{-12}$ fm^3.

The schematic picture of locations of roots and a region there $|\Delta_i(z)| \gtrsim 10^{-3}$ are presented in Fig.3.4. We see that the difference Δ_i is not essential in location of the roots and we can use the approximations (3.63) and (3.64).

The regularized version of the the function ψ is

$$\psi_{reg} = \psi_a(z)\Gamma_1 + \psi_b(z)\Gamma_2. \tag{3.66}$$

Now one has to put conditions (3.55) on the regularized functions

$$\frac{z_a}{2L}\,\frac{d}{dz}\psi_{reg}\Big|_{z=\tilde{z}_a} = 1 \tag{3.67}$$

$$\frac{z_b}{2L}\,\frac{d}{dz}\psi_{reg}\Big|_{z=\tilde{z}_b} = -1 \tag{3.68}$$

and find $\tilde{z}_a$ and $\tilde{z}_a$ from these conditions. However it is difficult to perform these calculations. Instead of finding $\tilde{z}_a$ from condition (3.109) we propose to use such regularization that does not change z_a found from formal conditions (3.55). We can check that the formal z_a in fact solves also the regularized condition if the regularization is smooth enough. So, we take z_a and substitute it in the LHS of regularized condition (3.109). We define

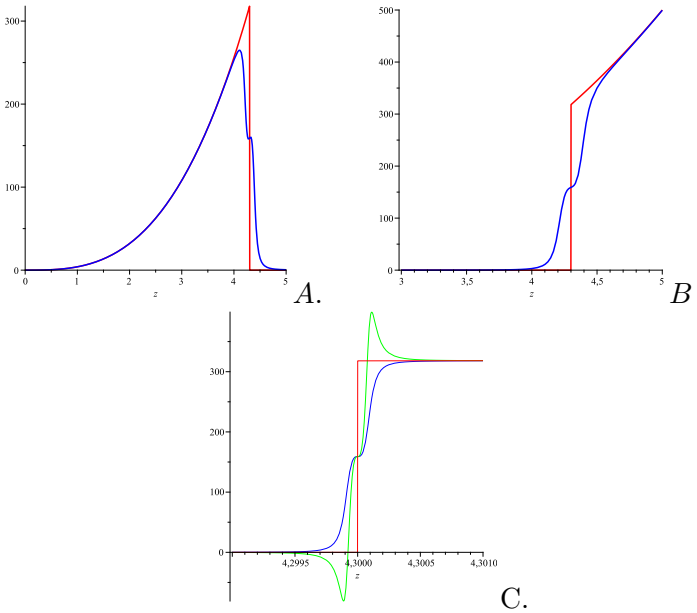

Figure 3.3. A. The functions $\frac{d\Upsilon_1}{dz}$(red line), $\left.\frac{d\widetilde{\Upsilon}_1}{dz}\right|_{appr}$ (blue line) . B. The functions $\frac{d\Upsilon_2}{dz}$ (red line), $\left.\frac{d\widetilde{\Upsilon}_2}{dz}\right|_{appr}$ (blue line). The regularization parameter $R = 10$ at A and B cases. C. Functions $\frac{d\Upsilon_2}{dz}$(red line), $\left.\frac{d\widetilde{\Upsilon}_2}{dz}\right|_{appr}$ (blue line) and $\frac{d\widetilde{\Upsilon}_2}{dz}$ (green line) at the regularization parameter $R = 10^4$.

$$F_{a,reg}\Big|_{z=z_a} = \frac{z_a}{2L}\left(\frac{d\psi_a}{dz}\Gamma_1 + \frac{d\psi_b}{dz}\Gamma_2\right)\Big|_{z=z_a} = 1+\delta_1,$$

$$F_{b,reg}\Big|_{z=z_b} = \frac{z_b}{2L}\left(\frac{d\psi_a}{dz}\Gamma_1 + \frac{d\psi_b}{dz}\Gamma_2\right)\Big|_{z=z_b} = -1+\delta_2.$$

We can calculate $F_{a,reg}$. The deviation of $F_{a,reg}$ from 1 will show how the regularization changes conditions (3.55). In the following table we present calculations of $F_{a,reg}$ for the wide range of parameter of the theory.

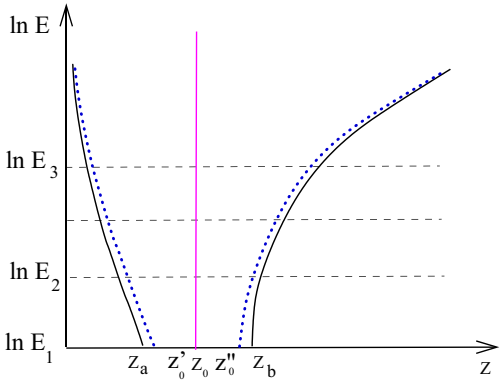

Figure 3.4. (color on-line) The schematic plots of locations of roots (solid black lines) dependent on the energy (in the logarithmic scale) and the location of differences $|\frac{d\widetilde{Y}_i}{dz} - (\frac{d\widetilde{Y}_i}{dz})_{appr}| \gtrsim 10^{-3}$, $i = 1, 2$ (the magenta shaded region). The magenta solid line shows the location of the wall. The dotted blue lines show location of zeros for the charged wall.

We choose the parameter R as minimally needed to make δ_1 and δ_2 negligible at energies $10^{-4} < E < 10^2$ TeV. Using the direct numerical calculations we choose $R = 10^4$. We perform numerical calculations at $R = 10^4$ and get the following table:

$E,\ TeV$	$Q,\ fm^{1/2}$	$z_a,\ fm$	$z_b, fm,$	F_a	F_b
118.2	0	0.044	$4.015 \cdot 10^6$	1.00000	−1.00000
30	0	0.069	$1.019 \cdot 10^6$	1.00000	−1.00000
0.03	0	0.695	1018.394	1.00000	−1.00000
0.00025	0	4.261	4.3404	0.99999	−0.99999

Thus, from the table evidently $F_a \approx 1$, $F_b \approx -1$.

As has been mentioned above, strictly speaking one may not consider infinite surface as a trapped surface of any kind. Nevertheless it is possible

to assume that transversal size of colliding objects is finite but very large, and therefore boundary conditions do not affect the process of gravitational interactions of inner parts of sources. If we are interested only in the specific area of the formed trapped surface in respect to the unit of shock wave area, we may define it as

$$\mathcal{A} \approx \lim_{L\to\infty} \frac{A_{trap}(L)}{A_{source}(L)}, \tag{3.69}$$

and the approximate equality takes place due to negligibility of boundary effects. As often happens, we can get answers for finite physical systems performing calculations for infinite non-physical objects.

3.3 Holographic QGP phase diagram for the central heavy-ions collisions

In this section we construct the phase diagram for TS formed in the central collision of two identical point-like charged shock waves [22].

The profile of point-like charged shock waves in AdS is given by (3.33) with (3.32) and (3.35). Existence of the trapped surface in the central collision of two point-like charged shock waves means the existence of a real solution, q_0, to the following equation (see [22] for details)

$$F'(q_0) - \frac{2}{1+2q_0}F(q_0) + \frac{2L}{\sqrt{q_0(1+q_0)}} = 0 \tag{3.70}$$

The left hand side of (3.70) can be written as

$$\mathcal{F}(L, E, \bar{Q}^2, q) = \frac{\mathcal{N}(L, \bar{M}, \bar{Q}^2, q)}{\mathcal{D}(a, q)}. \tag{3.71}$$

The numerator $\mathcal{N}(L, E, \bar{Q}^2, q)$ contains just one term with dependence on $\bar{Q}^2$. This dependence is linear with a positive coefficient

$$\mathcal{N}(a, \bar{M}, \bar{Q}^2, q) = \mathcal{N}(a, \bar{M}, q) + 15\frac{\pi}{a}\bar{Q}^2. \tag{3.72}$$

The denominator in (3.71) does not take infinite values. To find solutions to (3.70) for the shape function given by (3.33) we can draw the function

$$\begin{aligned} - \quad & \mathcal{N}(a, \bar{M}, q) \equiv -(512a^3q^5 + 1280a^3q^4 - \\ - \quad & 96\bar{M}\pi aq^2 + 1024a^3q^3 - 96\bar{M}\pi aq + 256a^3q^2), \end{aligned} \tag{3.73}$$

and see where this function can be equal to a given value $15\bar{Q}^2\frac{\pi}{a}$.

In order to find the maximal allowed $\bar{Q}^2$ at which solution to (3.70) still exists we find the maximum of function $\mathcal{N}$ for fixed energy,

$$\frac{d\mathcal{N}(a,\bar{M},q)}{dq}|_{q=q_{max}} = 0 \tag{3.74}$$

and the value

$$\frac{a}{15\pi}\mathcal{N}(a,\bar{M},q)|_{q=q_{max}}$$

defines $\bar{Q}^2_{max}$.

Let us remind that we are working in physical units and we use the following notations (3.37) and (3.36): $\bar{M} = \frac{4G_5E}{3\pi}$ and $\bar{Q}^2 = \frac{4G_5Q_n^2}{3\pi}$.

Results of calculations are presented in Fig. 3.5.

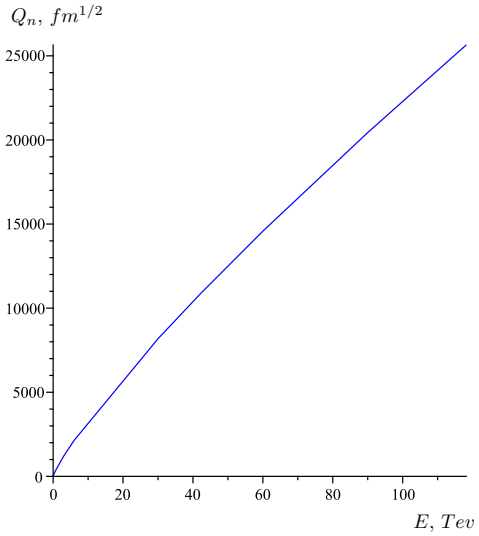

Figure 3.5. The allowed zone for the trapped surface formation is under the line on the diagram. The plot has been constructed by using formulas from [22].

To estimate corrections to GYP multiplicity due to non-zero chemical potential, we use formula (3.17) from [22]. In notations admitted in this paper, (3.32) and (3.35), the formula has the form

$$A_{AdS_5} \approx 4\pi L^3 \left(\frac{G_5 E}{L^2}\right)^{\frac{2}{3}} \left(1 - \frac{1}{24}\left(1 + \frac{5Q_n^2}{EL^2}\right)\left(\frac{2\sqrt{2}L^2}{G_5 E}\right)^{\frac{3}{2}}\right) \quad (3.75)$$

In Fig.3.6 we show the entropy, A_{AdS_5}, for $Q_n = 0$ and $Q_n \neq 0$. The blue line represents $Q_n = 0$. The red line represents $Q_n = 2 \cdot 10^6$. We see that the deviation form the GYP multiplicity is essential for small energies and is almost neglectful for large energies.

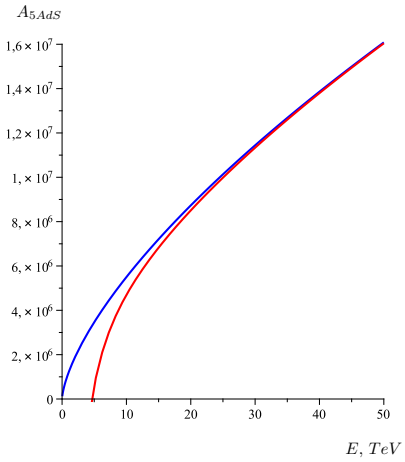

Figure 3.6. The function A_{AdS_5}, at $Q_n = 0$, (blue line) and $Q_n = 2 \cdot 10^6 fm^{1/2}$ (red line).

3.4 Holographic QGP phase diagram in the wall-wall dual model of heavy-ions collisions

3.4.1 Charged wall as a dual model for a heavy-ion

Let us note that the form of the J_{uu}^{WP} in (3.52) can be obtained by spreading out the energy-momentum tensor of an ultrarelativistic point, i.e J_{uu} in the form (3.25) with $\rho(q)$ given by eq.(3.31), over the transversal surface.

The Einstein equation for the charged wall (membrane) has the form

$$(\partial_z^2 - \frac{3}{z}\partial_z)\phi(z) = -16\pi G_5 \left(J_{uu}^{WP} + J_{uu}^{WQ}(Q,z) \right). \tag{3.76}$$

where J_{uu}^{WP} is given by (3.52) and we suppose that $J_{uu}^{WQ}(Q,z)$ can be obtained in the similar way by spreading the energy-momentum tenzor of the ultrarelativistic charged point T_{uu}^{pQ} over the transversal surface. In the previous calculations:

$$J_{uu}^{WQ} = \frac{\int_{\mathcal{M}} J_{uu}^{pQ} \mathcal{D}x_\perp}{\int_{\mathcal{M}} \mathcal{D}x_\perp} \tag{3.77}$$

here the subscript "pQ" means the electromagnetic part of the energy momentum tensor of the charged point particle and "$\mathcal{D}x_\perp$" means that we integrate over the induced metrics on the orthogonal surface $\mathcal{M}$.

For this purpose we take

$$J_{uu}^{pQ}(z,z_0) = \frac{L}{z}\rho^{pQ} \tag{3.78}$$

where ρ^{pQ} is given by (3.34), and according to our prescription (3.77) we integrate over all transversal coordinates

$$J_{uu}^{PQ,II} = \frac{\frac{L}{z}\int_0^\infty \rho^{pQ}(q)\frac{L^2}{z_0^2}\frac{1}{2}dr^2}{\int_0^\infty \frac{L^2}{z_0^2} r dr} \tag{3.79}$$

The result is

$$J_{uu}^{pQ} = \mathcal{X}\mathcal{J} \tag{3.80}$$

where

$$\mathcal{J} = \frac{64}{3} z z_0 \left(1 - \frac{z_0^6 - 3\,z^2 z_0^4 - 3\,z^4 z_0^2 + z^6}{|z_0^2 - z^2|^3} \right) \tag{3.81}$$

$$\mathcal{X} = \frac{5}{256}\frac{Q_n^2}{\pi L^6} = \frac{5}{256}\frac{Q^2}{L^6} \tag{3.82}$$

We see divergency at $z = z_0$, as it should be for the energy-momentum tensor of a charged plane. We introduce regularization by adding the ϵ factor in the denominator.

3.4.2 Charged wall-on-wall collision as a dual model for heavy-ions collisions

To find the TS formation condition in the wall-wall collision one has to solve Einstein equation

$$(\partial_z^2 - \frac{3}{z}\partial_z)\phi(z) = -16\pi G_5 \left(J_{uu}^{pW}(z) + J_{uu}^{QW}(Q,z) \right), \tag{3.83}$$

$$J_{uu}^{pW}(z) = \frac{E}{L^2}\frac{z_0^3}{L^3}\delta(z-z_0), \tag{3.84}$$

$$J_{uu}^{QW}(Q,z) = \frac{128\mathcal{X}}{3} z z_0 \frac{z^4\left(-z^2+3\,{z_0}^2\right)\theta(z_0-z) + z_0^4\left(-3z^2+z_0^2\right)\theta(z-z_0)}{\left(-z^2+z_0^2+\epsilon^2\right)^3} \tag{3.85}$$

with the following boundary conditions

$$\mathbf{1)} \qquad \phi(z_a) = \phi(z_b) = 0, \phi_a(z_0) = \phi_b(z_0) \tag{3.86}$$

$$\mathbf{2)} \qquad \left(\psi'(z_a)\frac{z_a}{L}\right) = 2, \quad \left(\psi'(z_b)\frac{z_b}{L}\right) = -2, \tag{3.87}$$

where z_a and z_b are the boundaries of the TS and ψ is related to

$$\phi(z) = \frac{z}{L}\psi. \tag{3.88}$$

We search for a solution to the Einstein equation with a charged source in the form of the sum of the "neutral" solution and a correction proportional to Q^2

$$\phi = \phi_n + \phi_q \tag{3.89}$$

here ϕ_n denotes the solution of the neutral case.

As in the neutral case it is convenient to consider domains $z < z_0$, $z > z_0$ separately

$$\phi_q = \begin{cases} \phi_{qz_0>z}, & z_0 > z; \\ \phi_{qz>z_0}, & z > z_0 \end{cases} \tag{3.90}$$

and we have

$$(\partial_z^2 - \frac{3}{z}\partial_z)\phi_q = -16\pi G_5 \mathcal{X}\frac{128}{3} z z_0 \frac{z^4\left(-z^2+3\,{z_0}^2\right)}{\left(-z^2+z_0^2+\epsilon^2\right)^3},\ z_0 > z \tag{3.91}$$

$$(\partial_z^2 - \frac{3}{z}\partial_z)\phi_q = -16\pi G_5 \mathcal{X}\frac{128}{3} z z_0 \frac{z_0^4\left(-3z^2+z_0^2\right)}{\left(-z^2+z_0^2-\epsilon^2\right)^3},\ z > z_0 \tag{3.92}$$

Solutions to (3.91) and (3.92) can be presented as :

$$\psi_{qz_0>z} = z^3 C_1 + \frac{C_2}{z} - \frac{NLz_0\, z^3}{4\left(-z^2 + {z_0}^2 + \epsilon^2\right)}, \quad z_0 > z, \tag{3.93}$$

$$\psi_{qz>z_0} = \frac{C_3}{z} + z^3 C_4 + \frac{NL{z_0}^5}{4z\left(-z^2 + {z_0}^2 + \epsilon^2\right)}, \quad z > z_0 \tag{3.94}$$

Here $N = \frac{40}{3}\frac{\pi G_5 Q^2}{L^6}$ The first two terms in (3.93) and (3.94) are solution to the Lin and Shuryak equation (55) in [18]. If one assumes that they satisfy condition **1**, i.e. $\psi_n(z_a) = \psi_n(z_b) = 0$, $\psi_{na}(z_0) = \psi_{nb}(z_0)$, one gets [60]:

$$\mathbf{\Psi}_n = \begin{cases} \psi_{na} = C\left(\dfrac{z^3}{z_a^3} - \dfrac{z_a}{z}\right), \; C = -\dfrac{4\pi G_5 E}{L^4}\dfrac{\left(\dfrac{z_0^4}{z_b^4} - 1\right) z_b}{\dfrac{z_b^4 - z_a^4}{z_a^3 z_b^3}}, \; z < z_0 \\ \\ \psi_{nb} = D\left(\dfrac{z^3}{z_b^3} - \dfrac{z_b}{z}\right), \; D = -\dfrac{4\pi G_5 E}{L^4}\dfrac{\left(\dfrac{z_0^4}{z_a^4} - 1\right) z_a}{\dfrac{z_b^4 - z_a^4}{z_a^3 z_b^3}}, \; z_0 < z \end{cases} \tag{3.95}$$

In the neutral case one find z_a and z_b from the 2-nd condition $\left(\psi'_{na}(z_a)\dfrac{z_a}{L}\right) = 2$, $\left(\psi'_{nb}(z_b)\dfrac{z_b}{L}\right) = -2$, here z_a and z_b are the boundaries of the TS.

As to (3.93) and (3.94), choosing

$$C_1 = \frac{NLz_0}{4(z_a^2 - z_0^2)}, \quad C_2 = 0, \tag{3.96}$$

$$C_3 = \frac{NLz_0^5}{4(z_b^2 - z_0^2)}, \quad C_4 = 0, \tag{3.97}$$

we obtain

$$\begin{cases} \psi_{aq} = -\dfrac{NLz_0 z^3}{4}\dfrac{-z_a^2 + z^2 - \epsilon^2}{(-z^2 + z_0^2 + \epsilon^2)(-z_a^2 + z_0^2)}, & z < z_0 \\ \\ \psi_{bq} = \dfrac{NLz_0^5}{4z}\dfrac{-z_b^2 + z^2 + \epsilon^2}{(-z^2 + z_0^2 - \epsilon^2)(-z_b^2 + z_0^2)}, & z_0 < z \end{cases} \tag{3.98}$$

Note that for the constructed solution the condition $\psi(z_a) = \psi(z_b) = 0$ is satisfied automatically.

The second requirement (3.87) gives

$$-\frac{8\pi G_5\, E\, (z_0^4 - z_b^4)\, z_a^3}{L^5(z_b^4 - z_a^4)} - \frac{N}{4}\frac{z_0 z_a^5}{(-z_a^2 + z_0^2)^2} = 1, \tag{3.99}$$

$$-\frac{8\pi G_5\, E\, (z_0^4 - z_a^4)\, z_b^3}{L^5(z_b^4 - z_a^4)} + \frac{N}{4}\frac{z_0^5 z_b}{(-z_b^2 + z_0^2)^2} = -1; \tag{3.100}$$

These equations do not have analytical solutions and we treat them numerically.

Roots of system (3.99),(3.100) could not be found analytically since these equations are equivalent to polynomial equations on z_a and z_b of a high degree (> 4). So we take $z_0 = L$ and analyze the following system numerically

$$F_a \equiv -\frac{8\pi G_5 E\, (z_0^4 - z_b^4)\, z_a^3}{z_0^5(z_b^4 - z_a^4)} - \frac{10}{3}\frac{\pi G_5 Q^2}{z_0^6}\frac{z_0 z_a^5}{(-z_a^2 + z_0^2)^2} = 1, \tag{3.101}$$

$$F_b \equiv -\frac{8\pi G_5 E\, (z_0^4 - z_a^4)\, z_b^3}{z_0^5(z_b^4 - z_a^4)} + \frac{10}{3}\frac{\pi G_5 Q^2}{z_0^6}\frac{z_0^5 z_b}{(-z_b^2 + z_0^2)^2} = -1 \tag{3.102}$$

To show the movement of roots of equations (3.101) and (3.102) we suppose that z_b for given Q is already known and represent function $F_a(z_a, z_b)$ as function of z_a in Fig. 3.7. In the similar way, supposing that z_a is already known we represent function $F_b(z_a, z_b)$ as function of z_b in Fig. 3.8.

In Fig.3.9 we show the charge flows of the roots. Different lines correspond to different energies. We see that the flows go to z_0 and reach the line $z = z_0$ for $Q = Q_{cr}$. In Fig.3.10 we draw the corresponding flow for physical parameters.

3.4.3 Comparison of the results

It is interesting to compare the phase diagrams, the energy (temperature) E vs the charge (chemical potential) Q, corresponding to the pointlike charge and the spread charge. Results of these calculations are collected in the table below and presented in Fig.3.11. We see that this two phase diagrams are qualitatively the same.

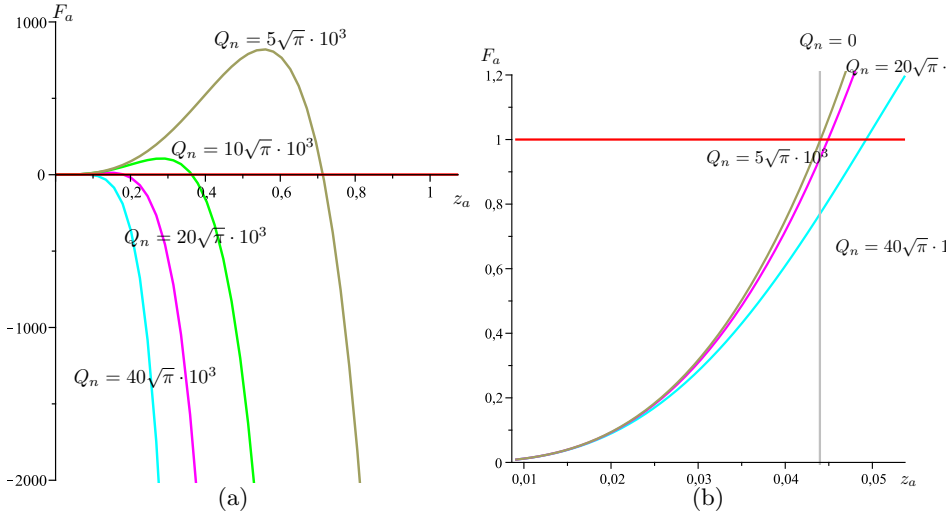

Figure 3.7. (a) The plot of $F_a(z_a, z_b)$ as a function of z_a for fixed z_b near the root $z_a = z_a(E)$ at $E = 118.2$ TeV. (b) Zooming in the region of small F_a and small z_a.

E (TeV)	118.2	60	30	6	3
$Q_{cr,\,point}$	25649.6	14577.2	8180.6	2138.7	1199.9
$Q_{cr,\,wall}$	47500	27000	15170	3950	2220
E (TeV)	0.6	0.06	0.03	0.0003	0.00025
$Q_{cr,\,point}$	313.3	45.6	25.4	0.43	0.37
$Q_{cr,\,wall}$	570	80	40	0.15	0

From Fig. 3.11 it is evident that the two lines, the red and the blue ones, have a cross point. We represent the cross point in natural and logarithmic scales in Fig. 3.12.

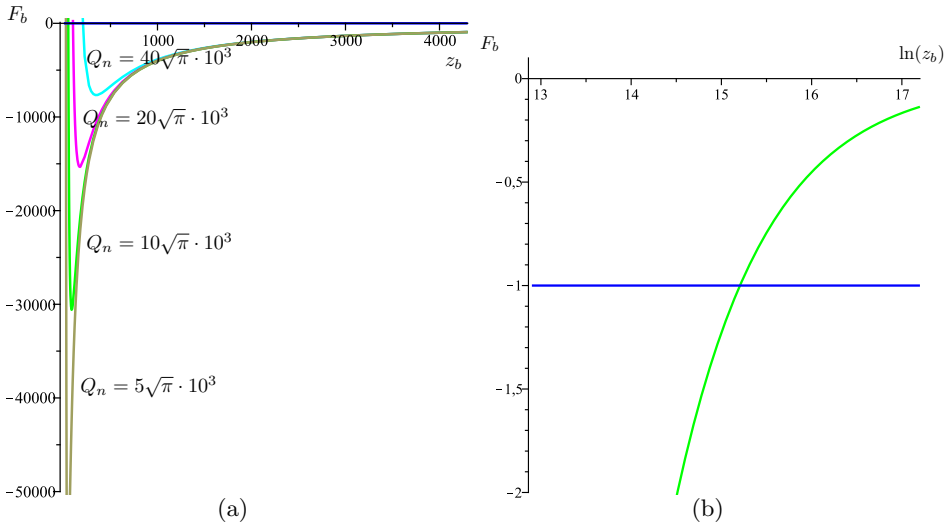

Figure 3.8. (a) The plot of $F_b(z_a, z_b)$ as a function of z_b for fixed z_a near the root $z_b(E)$ at $E = 118.2$ TeV. (b) Zooming in the region of small negative F_b and presenting z_b in the logarithmic scale.

3.4.4 The square trapped surface calculation

Following [18] we calculate entropy lower bound as "the area of the trapped surface" per an unite square of the wall[3] using the formula:

$$S = \frac{2A}{4G_5} = \frac{\int \sqrt{g} dz d^2x_\perp}{2G_5}, \tag{3.103}$$

$$s \equiv \frac{S}{\int d^2x_\perp} = \frac{L^3}{4G_5}\left(\frac{1}{z_a^2} - \frac{1}{z_b^2}\right). \tag{3.104}$$

In the absence of transverse dependence one ignores $x_\perp^2$ in (3.103). (3.104) measures entropy per transverse area.

The trapped surface decreases with growth of a charge. The corresponding graphical representations are in Fig. 3.13.

In Fig.3.14 we show the entropy per volume given by (3.104) as function of energy for different Q. This plot is similar to the plot presented

[3] We put "area" and "trapped surface" in quotation marks since in the strict notions of the trapped surface it has to be smooth and compact. In our case it is not smooth and it does not have finite area, one can only assume this properties after regularization

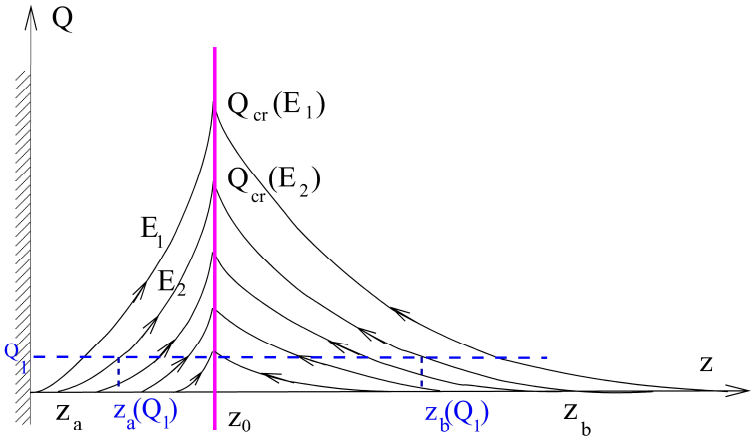

Figure 3.9. The schematic picture of charge flows. The magenta solid line shows the position of the wall. We see that the positions of points $z_a(Q)$ and $z_b(Q)$ move to the point $z = z_0$ when we increase Q. For $Q \to Q_{cr}(E)$ the segment $[z_a(Q), z_b(Q)]$ shrinks to zero.

in Fig. 3.6. We see that the influence of the chemical potential on the multiplicity is essential for small energies and is almost neglectful for large energies.

3.4.5 Remarks about the regularization

The regularized version of the the function ψ is

$$\psi_{reg} = \psi_a(z)\Gamma_1 + \psi_b(z)\Gamma_2 \tag{3.105}$$

where $\psi_a(z)$ and $\psi_b(z)$ define the function ψ without regularization,

$$\psi = \psi_a(z)\Theta(z_0 - z) + \psi_b(z)\Theta(z - z_0) \tag{3.106}$$

$$\psi_a(z) = -\frac{4\,G\pi\,E\left(\frac{z_0^4}{{z_b}^4} - 1\right){z_b}^4{z_a}^3\left(\frac{z^3}{{z_a}^3} - \frac{z_a}{z}\right)}{L^4\left({z_b}^4 - {z_a}^4\right)} - \frac{10}{3}\,\frac{Q^2 G\pi\, z_0\, z^3\left(-{z_a}^2 + z^2\right)}{L^5\left(-z^2 + {z_0}^2\right)\left(-{z_a}^2 + {z_0}^2\right)}$$

$$\psi_b(z) = -\frac{4\,G\pi\,E\left(\frac{z_0^4}{{z_a}^4} - 1\right){z_a}^4{z_b}^3\left(\frac{z^3}{{z_b}^3} - \frac{z_b}{z}\right)}{L^4\left({z_b}^4 - {z_a}^4\right)} + \frac{10}{3}\,\frac{Q^2 G\pi\, {z_0}^5\left(-{z_b}^2 + z^2\right)}{L^5 z\left(-z^2 + {z_0}^2\right)\left(-{z_b}^2 + {z_0}^2\right)}$$

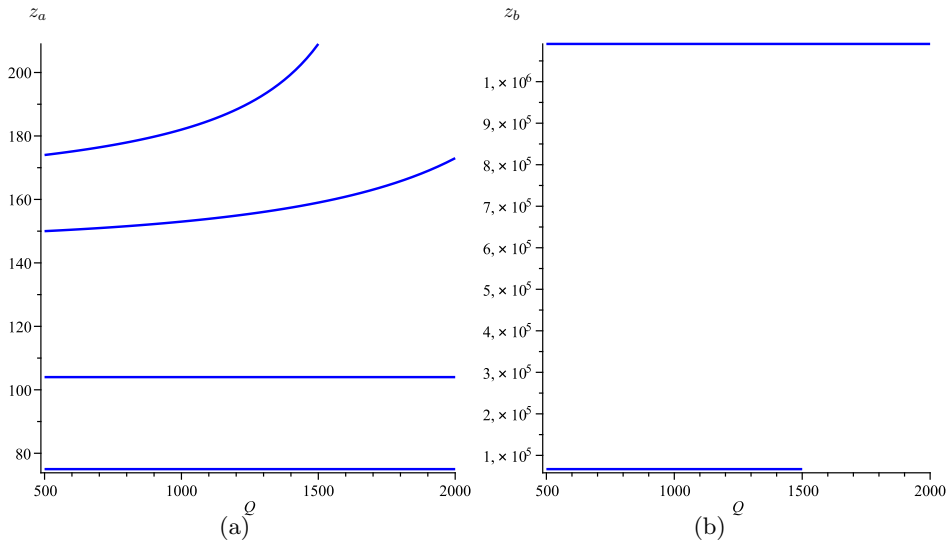

Figure 3.10. (a) The charge flows of the root $z_a(Q)$ for $E = 1.97\,\text{TeV}$, $3\,\text{TeV}$, $9\,\text{TeV}$, and $24\,\text{TeV}$. (b) The charge flows of the roots $z_b(Q)$ for $E = 1.97\,\text{TeV}$, $3\,\text{TeV}$.

and

$$\Gamma_1 = \frac{\arctan\left(R\left(z_0 - z\right)\right)^3}{\pi} + \frac{1}{2} \tag{3.107}$$

$$\Gamma_2 = \frac{\arctan\left(R\left(z - z_0\right)\right)^3}{\pi} + \frac{1}{2} \tag{3.108}$$

Now one has to put conditions (3.55) on the regularized functions

$$\frac{z_a}{2L}\,\frac{d}{dz}\psi_{reg}\Big|_{z=\tilde{z}_a} = 1 \tag{3.109}$$

However it is difficult to find $\tilde{z}_a$ from the condition (3.109). Instead of finding $\tilde{z}_a$ from the condition (3.109) we propose to use such regularization that does not change z_a found from the formal conditions (3.55). We can check that the formal z_a in fact solves also the regularized condition if the regularization is smooth enough. So, the take z_a and substitute it in the LHS of the regularized condition (3.109). We define

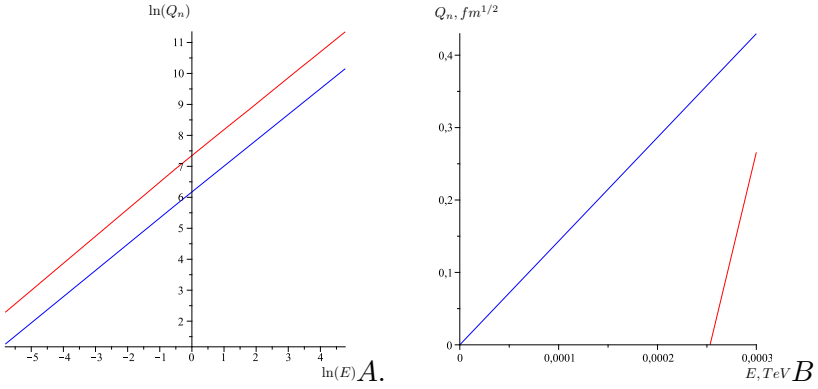

Figure 3.11. A. The phase diagram the logarithm of Q_n vs the logarithm of E at large E. B. The phase diagram E vs Q_n for small E and small Q_n. The blue lines correspond to the pointlike charge and the red lines to the spread charge. The zones above the lines are forbidden for black holes production for corresponding E and Q.

$$F_{a,reg}\Big|_{z=z_a} = \frac{z_a}{2L}\left(\frac{d\psi_a}{dz}\Gamma_1 + \frac{d\psi_b}{dz}\Gamma_2\right)\Big|_{z=z_a} \approx 1,$$

$$F_{b,reg}\Big|_{z=z_b} = \frac{z_b}{2L}\left(\frac{d\psi_a}{dz}\Gamma_1 + \frac{d\psi_b}{dz}\Gamma_2\right)\Big|_{z=z_b} \approx -1.$$

We can calculate $F_{a,reg}$ and $F_{b,reg}$. In the following table we present calculations of $F_{a,reg}$ and $F_{b,reg}$ for the wide range of parameter of the theory. Results of calculations at $R = 10^4$ are presented in the following table:

$E,\ TeV$	$Q = Q_n/\sqrt{\pi},\ fm^{1/2}$	$z_a,\ fm$	$z_b, fm,$	F_a	F_b
118.2	40000	0.049	$4.015 \cdot 10^6$	0.99997	−1.00000
3	15000	0.088	$1.019 \cdot 10^6$	1.00000	−1.00000
0.03	40	0.786	1017.792	1.00000	−1.00000

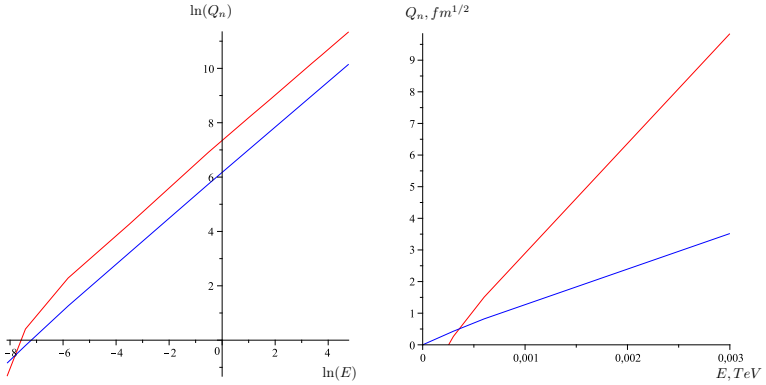

Figure 3.12. The cross point of two diagrams in logarithmic and natural scales.

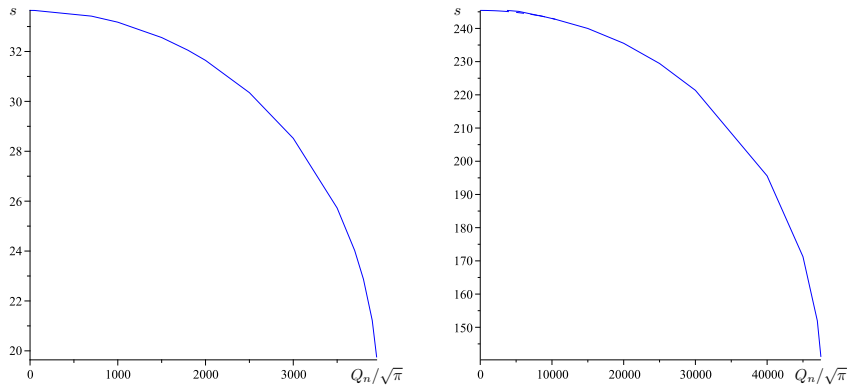

Figure 3.13. The dynamics of the trapped surface area $s(Q_n/\sqrt{\pi})$ at $E = 6\,TeV$, $E = 118.2\,TeV$.

Thus, from the table it is evident that $F_a \approx 1$, $F_b \approx -1$.

3.5 Conclusion

3.5.1 Summary

In this chapter we have constructed the phase diagram of the quark gluon plasma (QGP) formed at a very early stage just after the heavy ion collision. In this construction we have used a holographic dual model for the heavy ion collision. In this dual model colliding ions are described by the charged shock gravitational waves. Points on the phase diagram

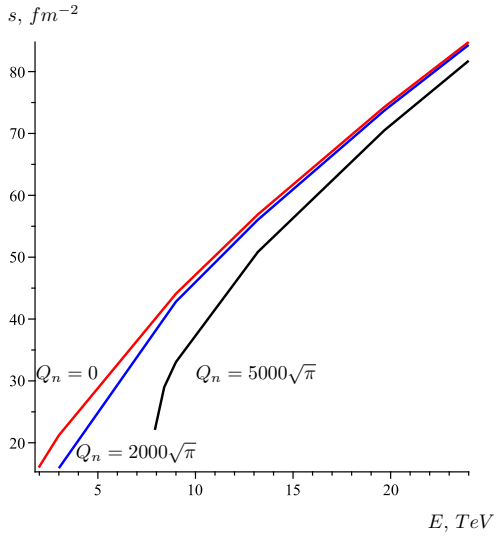

Figure 3.14. The red line corresponds to the case $Q_n = 0\, fm^{1/2}$, the blue to the case $Q_n = 2000\sqrt{\pi}\, fm^{1/2}$, the black to the case $Q_n = 5000\sqrt{\pi}\, fm^{1/2}$.

correspond to the QGP or hadronic matter with given temperatures and chemical potentials. The phase of QGP in dual terms is related to the case when the collision of shock waves leads to formation of trapped surface. Hadronic matter and other confined states correspond to the absence of trapped surface after collision.

Multiplicity of the ion collision process has been estimated in the dual language as an area of the trapped surface. We have shown that a non-zero chemical potential reduces the multiplicity. To plot the phase diagram we use two different dual models of colliding ions. The first model uses the point shock waves and the second the wall shock waves. We have found qualitative agrement of the results.

A special attention has been devoted to a regularization procedure for calculations performed for wall shock waves. On the one hand technically these calculations are essential simpler, but on the other hand, this approach, strictly speaking, is incorrect and requires a regularization. We have shown that a natural regularization does exist. Moreover, the proposed regularization does not make calculations to be more complicated as compare with naive (direct) calculations. This open new possibility for simple calculations for wall shock waves bearing nontrivial matter charges.

3.5.2 Further directions

Head-on collisions of point charged shock waves have only two parameters. In the dual language they correspond to energy and chemical potential per nucleus. Off-center collisions are also specified by the impact parameter and the change of this parameter can be associated with a dual change from "non-thermal" peripheral to "thermal" central collisions [18]. However, this is still an oversimplification of the problem. The physics of heavy-ion collision in RHIC is richer and as indicated in [18, 60], rapid equilibration and hydrodynamical behavior experimentally observed at RHIC for collisions of two heavy ions such as AuAu, does not have the place for deuteron-Au collisions at the same rapidity. Maybe it is too naive to believe that the simplest shock wave related by a boost to the Schwarzschild black hole in AdS can mimic the nuclear matter in the colliders. However this simple shock wave in fact reproduces the interaction of a relativistic quark with gravity and by this reason, may be considered as a simplest candidate to mimic the nuclear matter within the holographic conjecture. One can try to associate different nuclei with different forms of shock waves. Let us remind in this context that the form of the shock wave follows from the eikonal approximation of the gravity-quark interaction in 5-dimension [61, 26]. The presence of the electromagnetic field or other fields as well as any improvements of the eikonal approximation for sure changes the form of the shock waves and it would be interesting to see holographical consequences of this consideration.

The obtained lower bound on N_{charged} scales as $s_{NN}^{1/3}$, which is a faster energy dependence than the $s_{NN}^{1/4}$ scaling predicted by the Landau model [37] and largely obeyed by the data. If one has a priory a restriction on allowed energy then one can fit constants to guaranty that the experimental data are above the AdS bound. Note that taking into account the chemical potential permits to increase the allowed energy. However one cannot expect to much from the chemical potential corrections. The relevant chemical potential for baryon number is not expected to be large, i.e. $\mu_B \sim 30MeV$ or $\mu_B/T \sim 0.15$ for recent experiments at RHIC [62] and so any effects will be limited. However, as has been mentioned in the text, the relation between the value of chemical potential and the value of the 5-dimentional charge is in our disposal and we can assume a huge ratio of them.

It would be also interesting to try to use plane gravitational waves in AdS_5 to describe nonperturbative stages in the gauge theories and colli-

sions of these waves to describe the QGP formed in the heavy ions collisions. In the plane case, the Chandrasekhar-Ferrari-Xanthopoulos duality between colliding plane gravitational waves and the Kerr black hole solution, has been used as a model of the BH formation [63]. It would be interesting to generalize this duality to the AdS case. This may get a new insight to a possible dependence of multiplicities on the rapidity.

Bibliography

[1] J. M. Maldacena, Adv. Theor. Math. Phys. 2, 231 (1998) [Int. J. Theor. Phys. 38, 1113 (1999)]; arXiv:hep-th/9711200.

[2] S. S. Gubser, I. R. Klebanov and A. M. Polyakov, Phys. Lett. B 428, 105 (1998) ; arXiv:hep-th/9802109.

[3] E. Witten, Adv. Theor. Math. Phys. 2, 253 (1998); arXiv:hep-th/9802150.

[4] G. Policastro, D. T. Son and A. O. Starinets, "The Shear viscosity of strongly coupled N=4 supersymmetric Yang-Mills plasma," Phys. Rev. Lett. **87**, 081601 (2001); hep-th/0104066.

[5] J. Casalderrey-Solana, H. Liu, D. Mateos, K. Rajagopal, and U. A. Wiedemann, *Gauge/String Duality, Hot QCD and Heavy Ion Collisions*, arXiv:1101.0618.

[6] A. Bernamonti and R. Peschanski, *Time-dependent AdS/CFT correspondence and the Quark-Gluon Plasma*, arXiv:1102.0725.
R. A. Janik *The dynamics of quark-gluon plasma and AdS/CFT*, Lectures at the 5th Aegean summer school, "From gravity to thermal gauge theories: the AdS/CFT correspondence", Adamas, Milos Island, Greece, September 21-26, 2009; arXiv:1003.3291

[7] E. Shuryak, Prog. Part. Nucl. Phys. 53, 273 (2004); arXiv:hep-ph/0312227.

[8] E. V. Shuryak, Nucl. Phys. A 750, 64 (2005); arXiv:hep-ph/0405066.

[9] U. W. Heinz, AIP Conf. Proc. 739, 163 (2004); arXiv:nucl-th/0407067.

[10] R. A. Janik and R. B. Peschanski, Phys. Rev. D 74, 046007 (2006); arXiv:hep-th/0606149.
R. A. Janik and R. Peschanski, Phys. Rev. D 73, 045013 (2006); arXiv:hep-th/0512162.

[11] S.S. Gubser, S.S. Pufu and A. Yarom, *Entropy production in collisions of gravitational shock waves and of heavy ions*, Phys.Rev., D 78 (2008) 066014; arXiv: 0805.1551.

[12] H. Nastase, "On high energy scattering inside gravitational backgrounds," hep-th/0410124.

[13] H. Nastase, "The RHIC fireball as a dual black hole," hep-th/0501068.

[14] E. Shuryak, S.-J. Sin, and I. Zahed, "A gravity dual of RHIC collisions," J. Korean Phys. Soc. 50 (2007) 384–397; hep-th/0511199.

[15] A. J. Amsel, D. Marolf, and A. Virmani, "Collisions with Black Holes and Deconfined Plasmas," JHEP **04** (2008) 025; arXiv:0712.2221.

[16] D. Grumiller and P. Romatschke, "On the collision of two shock waves in AdS5," arXiv:0803.3226.

[17] S.S. Gubser, S.S. Pufu and A. Yarom, Off-center collisions in AdS5 with applications to multiplicity estimates in heavy-ion collisions JHEP **11** (2009)050; arXiv:0902.4062.

[18] S. Lin, E. Shuryak, Grazing Collisions of Gravitational Shock Waves and Entropy Production in Heavy Ion Collision; arXiv:0902.1508.

[19] A. Duenas-Vidal and M. A. Vazquez-Mozo, "Colliding AdS gravitational shock waves in various dimensions and holography," JHEP **1007**, 021 (2010); arXiv:hep-th/1004.2609.

[20] L. Alvarez-Gaume, C. Gomez, A. S. Vera, Al. Tavanfar, M. A. Vazquez-Mozo, *Critical formation of trapped surfaces in the collision of gravitational shock waves*, JHEP **0902**, 009 (2009); arXiv:0811.3969.

[21] S. S. Gubser, A. Nellore, "Mimicking the QCD equation of state with a dual black hole," Phys. Rev. **D78** (2008) 086007; arXiv:0804.0434.

[22] I. Y. Aref'eva, A. A. Bagrov and L. V. Joukovskaya, "Critical Trapped Surfaces Formation in the Collision of Ultrarelativistic Charges in (A)dS," JHEP **1003** , 002, (2010); arXiv:hep-th/0909.1294.

[23] H.Yoshino and R. B. Mann, Black hole formation in the head-on collision of ultrarelativistic charges, arXiv:0605131.

[24] U. Gursoy and E. Kiritsis, "Exploring improved holographic theories for QCD: Part I," JHEP **0802** (2008) 032; arXiv: 0707.1324.
U. Gursoy, E. Kiritsis and F. Nitti, *"Exploring improved holographic theories for QCD: Part II,"* JHEP **0802** (2008) 019; arXiv: 0707.1349.

[25] E. Kiritsis, A. Taliotis, "Multiplicities from black-hole formation in heavy-ion collisions", arxiv:1111.1931.

[26] I.Ya. Aref'eva, Catalysis of Black Holes/Wormholes Formation in High Energy Collisions, Physics of Particles and Nuclei, 41 (2010), 835, arXiv: 0912.5481.

[27] D. Mateos, S. Matsuura, R. C. Myers, and R. M. Thomson, "Holographic phase transitions at finite chemical potential", JHEP **11** (2007) 085,; arXiv:0709.1225

[28] S. Kobayashi, D. Mateos, S. Matsuura, R.C. Myers and R.M. Thomson, "Holographic phase transitions at finite baryon density," JHEP **0702**, 016 (2007); arXiv:hep-th/0611099.

[29] Koji Hashimoto, Norihiro Iizuka, and Takashi Oka, Rapid Thermalization by Baryon Injection in Gauge/Gravity Duality; arXiv:1012.4463

[30] R. C. Myers, M. F. Paulos, A. Sinha, "Holographic Hydrodynamics with a Chemical Potential," JHEP **0906**, 006 (2009); arXiv: 0903.1596

[31] S. Hands, T. J. Hollowood, and J. C. Myers, QCD with Chemical Potential in a Small Hyperspherical Box, JHEP **1007**, 086 (2010); arXiv:1003.5813.

[32] N. Horigome and Y. Tanii, Holographic chiral phase transition with chemical potential, JHEP **01** (2007) 072,; hep-th/0608198.

[33] A. Parnachev, Holographic QCD with Isospin Chemical Potential, JHEP 02, 062 (2008); arXiv:0708.3170.

[34] J. Erdmenger, M. Haack, M. Kaminski and A. Yarom, "Fluid dynamics of R-charged black holes," JHEP **0901**, 055 (2009); arXiv:hep-th/0809.2488.

[35] S. W. Hawking and D. N. Page, Thermodynamics of Black Holes in anti-De Sitter Space, Commun. Math. Phys. 87 (1983) 577.

[36] S. S. Gubser, I. R. Klebanov, and A. W. Peet, "Entropy and Temperature of Black 3-Branes," Phys. Rev. D54 (1996) 3915–3919; hep-th/9602135.

[37] L. D. Landau, "On the multiparticle production in high-energy collisions," Izv. Akad. Nauk Ser. Fiz. **17**, 51 (1953) (in Russian). [English translation: *Collected Papers of L. D. Landau, edited by D. ter Haar (Gordon and Breach, New-York, 1968)*].

[38] J. D. Bjorken, "Highly Relativistic Nucleus-Nucleus Collisions: The Central Rapidity Region," Phys. Rev. D **27**, 140 (1983).

[39] C. Fefferman and C.R. Graham, "Conformal Invariants," in *Elie Cartan et les Mathématiques d'aujourd'hui*, Astérisque (1985) 95.

[40] A. Chamblin, R. Emparan, C. V. Johnson and R. C. Myers, "Charged AdS black holes and catastrophic holography," Phys. Rev. D **60**, 064018 (1999); arXiv:hep-th/9902170.
A. Chamblin, R. Emparan, C. V. Johnson and R. C. Myers, "Holography, thermodynamics and fluctuations of charged AdS black holes," Phys. Rev. D **60**, 104026 (1999); arXiv:hep-th/9904197.

[41] C. S. Peca and J. P. S. Lemos, "Thermodynamics of Reissner-Nordstroem-anti-de Sitter black holes in the grand canonical ensemble," Phys. Rev. D **59**, 124007 (1999); arXiv:gr-qc/9805004.
M. Cvetic and S. S. Gubser, "Phases of R-charged black holes, spinning branes and strongly coupled gauge theories," JHEP **9904**, 024 (1999); arXiv:hep-th/9902195.

[42] K. Skenderis, Lecture notes on holographic renormalization, Class. Quant. Grav. 19 (2002) 5849; hep-th/0209067.

[43] I. Y. Aref'eva and I. V. Volovich, "On the breaking of conformal symmetry in the AdS/CFT correspondence," Phys. Lett. B **433**, 49 (1998); arXiv:hep-th/9804182.

[44] M. Hotta and M. Tanaka, "Shock wave geometry with nonvanishing cosmological constant," Class. Quant. Grav. **10** (1993) 307–314.

[45] K. Sfetsos, "On gravitational shock waves in curved space-times," Nucl. Phys. **B436** (1995) 721–746; hep-th/9408169.

[46] G. T. Horowitz and N. Itzhaki, "Black holes, shock waves, and causality in the AdS/CFT correspondence," JHEP **02** (1999) 010; hep-th/9901012.

[47] R. Emparan, "Exact gravitational shockwaves and Planckian scattering on branes," Phys. Rev. **D64** (2001) 024025; hep-th/0104009.

[48] J. Podolsky and J. B. Griffiths, "Impulsive waves in de Sitter and anti-de Sitter space-times generated by null particles with an arbitrary multipole structure," Class. Quant. Grav. 15 (1998) 453–463; gr-qc/9710049.

[49] I. Y. Aref'eva, A. A. Bagrov and E. A. Guseva, "Critical Formation of Trapped Surfaces in the Collision of Non-expanding Gravitational Shock Waves in de Sitter Space-Time," JHEP **0912**, 009 (2009); arXiv:hep-th/0905.1087.

[50] R. Penrose, unpublished, 1974.

[51] D. M. Eardley and S. B. Giddings, Phys. Rev. D 66, 044011 (2002); arXiv:gr-qc/0201034.

[52] N. Kaloper and J. Terning, "How black holes form in high energy collisions," Gen. Rel. Grav. **39**, 1525 (2007) [Int. J. Mod. Phys. D **17**, 665 (2008)]; arXiv:hep-th/0705.0408.

[53] S.W. Hawking and G.R.E Ellis, The large scale structure of space-time (Cambridge Univ. Press, Cambridge, 1973).
R.M. Wald, General relativity (The University of Chicago Press, Chicago, 1984).

[54] S. Klein and J. Nystrand, *"Exclusive vector meson production in relativistic heavy ion collisions,"* Phys. Rev. **C60** (1999) 014903; hep-ph/9902259.

[55] **STAR** Collaboration, J. Adams et. al., *"Production of e+ e- pairs accompanied by nuclear dissociation in ultra-peripheral heavy ion collision,"* Phys. Rev. **C70** (2004) 031902; nucl-ex/0404012.

[56] S. Ochs, U. W. Heinz, "Entropy production by resonance decays," Phys. Rev. **C54**, 3199–3211 (1996); hep-ph/9606458.

[57] F. Karsch, "Lattice QCD at high temperature and density," Lect. Notes Phys. **583** (2002) 209–249; hep-lat/0106019.

[58] B. Muller, A. Schafer, "Entropy Creation in Relativistic Heavy Ion Collisions,", arXiv: 1110.2378

[59] B. B. Back et. al., "The significance of the fragmentation region in ultrarelativistic heavy ion collisions," Phys. Rev. Lett. **91** (2003) 052303; nucl-ex/0210015.

[60] S. Lin, E. Shuryak, Phys.Rev. D, **83**, 045025 (2011); arXiv: 1011.1918.

[61] G. 't Hooft, Phys. Lett. B 198 (1987); Nucl. Phys. B 304 (1988) 867.

[62] S. Ghosh, S. Sarkar and J. Alam, "Observing many body effects on lepton pair production from low mass enhancement and flow at RHIC and LHC energies," Eur. Phys. J. C **71**, 1760 (2011); arXiv:1009.1260.

[63] I.Ya. Aref'eva, K.S. Viswanathan, and I.V. Volovich, *Planckian-energy scattering, colliding plane gravitational waves and black hole creation*, Nucl. Phys. B 452 (1995) 346.